Stopped-Flow Fluorescence Studies of HMG-Domain Protein Binding to Cisplatin-Modified DNA†

Elizabeth R. Jamieson and Stephen J. Lippard*

Department of Chemistry, Massachusetts Institute of Technology, Cambridge, Massachusetts 02139

Received February 14, 2000; Revised Manuscript Received May 12, 2000

ABSTRACT: High-mobility group (HMG) domain proteins bind specifically to the major DNA adducts formed by the anticancer drug cisplatin and can modulate the biological response to this inorganic compound. Stopped-flow fluorescence studies were performed to investigate the kinetics of formation and dissociation of complexes between HMG-domain proteins and a series of 16-mer oligonucleotide probes containing both a 1,2-intrastrand d(GpG) cisplatin cross-link and a fluorescein-modified deoxyuridine residue. Rate constants, activation parameters, and dissociation constants were determined for complexes formed by HMG1 domain A and the platinated DNA probes. The sequence context of the cisplatin adduct modulates the value of the associative rate constant for HMG1 domain A by a factor of 2−4, contributing significantly to differences in binding affinity. The rates of association or dissociation of the protein−DNA complex were similar for a 71 bp platinated DNA analogue. Additional kinetic studies performed with HMG1 domain B, an F37A domain A mutant, and the full-length HMG1 protein highlight differences in the binding properties of the HMG domains. The stopped-flow studies demonstrate the utility of the fluorescein−dU probe in studying protein−DNA complexes. The kinetic data will assist in determining what role these proteins might play in the cisplatin mechanism of action.

Protein-platinated DNA complexes can mediate biological responses to the anticancer drug cisplatin[1] (*1, 2*), which is used to treat a variety of human malignancies, including testicular, ovarian, and cervical tumors (*3, 4*). The biological activity of this drug stems from its ability to bind DNA, where it forms predominantly 1,2-intrastrand cross-links with the platinum bound to the N7 positions of adjacent purine bases (*5*). These adducts distort DNA structure by inducing bending and unwinding of the duplex and can inhibit replication and transcription (*1, 2*). The recognition of the DNA adducts by cellular proteins is presumed to be an important step in the mechanism of action (*1, 2*).

A leading class of proteins proposed to participate in the cisplatin mechanism is the high-mobility group (HMG) domain protein family (*2*). These proteins contain at least one homologous 80-amino acid DNA-binding motif known as an HMG domain (*6*). Some HMG-domain proteins function as transcription factors, whereas others serve as chromatin architectural components (*6*). HMG-domain proteins bind DNA in the minor groove, recognizing specific DNA sequences and/or distorted DNA structures, including the cisplatin 1,2-intrastrand cross-link (*6*). In addition to their binding specificity, they inhibit the repair of cisplatin−DNA adducts in vitro and in vivo (*7−10*), suggesting one possibility for how these proteins could modulate the biological response to cisplatin.

The interaction between HMG-domain proteins and cisplatin-modified DNA has been examined in many studies that have focused on thermodynamic issues, revealing information about their binding affinities for cisplatin-modified DNA (*11−17*). The dissociation constants for these complexes can vary by orders of magnitude depending on the HMG-domain protein itself and the DNA sequence flanking the cisplatin adduct (*13*). In contrast, kinetic parameters that characterize the formation of these protein−DNA complexes have only just begun to be examined. A stopped-flow study using fluorescence resonance energy transfer (FRET) techniques revealed the binding of HMG1 domain B to cisplatin-modified DNA to be diffusion-controlled (*18*). Fluorescence stopped-flow kinetic studies performed here provide additional information concerning the interaction between HMG1 domains A and B and DNA probes with a 1,2-intrastrand d(GpG) cisplatin−DNA adduct and a fluorescein-modified deoxyuridine (dU) residue. In particular, the dependence of the kinetic parameters on the DNA sequence context of the cisplatin adduct and on the length of the oligonucleotide was examined. The results obtained highlight differences between the DNA binding properties of HMG1 domains A and B.

Detailed kinetic information has been obtained for many protein−DNA complexes by using stopped-flow fluorescence techniques. Often, these types of studies monitor changes in intrinsic protein fluorescence (*19−21*) and fluorescence

† This work was supported by Grant CA34992 (S.J.L.) from the National Cancer Institute. E.R.J. is a recipient of a Wyeth-Ayerst American Chemical Society Division of Medicinal Chemistry Predoctoral Fellowship.

* To whom correspondence should be addressed: Department of Chemistry, Massachusetts Institute of Technology, 77 Massachusetts Ave., Cambridge, MA 02139. Phone: (617) 253-1892. Fax: (617) 258-8150. E-mail: lippard@lippard.mit.edu.

[1] Abbreviations: HMG, high-mobility group; cisplatin, *cis*-diamminedichloroplatinum(II); FRET, fluorescence resonance energy transfer; HEPES, *N*-(2-hydroxyethyl)piperazine-*N*′-2-ethanesulfonic acid; Tris, tris(hydroxymethyl)aminomethane; HPLC, high-performance liquid chromatography; BSA, bovine serum albumin; DTT, dithiothreitol.

10.1021/bi000342h CCC: $19.00
Published on Web 06/24/2000

anisotropy (*22*) or changes that occur due to FRET (*23*, *24*). The experiments performed here monitor fluorescence changes from a fluorescein molecule, attached to a deoxyuridine and located in the major groove, upon protein binding in the minor groove of DNA. Similar studies were performed to investigate netropsin binding to a DNA dodecamer (*25*, *26*) and the interaction of UvrA and UvrB with DNA damaged by tetramethylrhodamine−dU (*27*). The kinetic parameters obtained from these stopped-flow fluorescence experiments complement the results of studies that use techniques such as gel mobility shift assays to gain thermodynamic information about protein−DNA complexes.

The kinetic data also pertain to the question of how HMG-domain proteins might help sensitize cells to cisplatin. The rates of formation and dissociation of different protein−DNA complexes, not only binding affinities, are important in any proposed mechanism. Competition between various protein−DNA complexes could be kinetically controlled, making it important to delineate this aspect of complex formation. Pooling the information from thermodynamic and kinetic studies provides a more detailed understanding of the protein−DNA complexes and allows one to determine whether a proposed mechanism of action is reasonable.

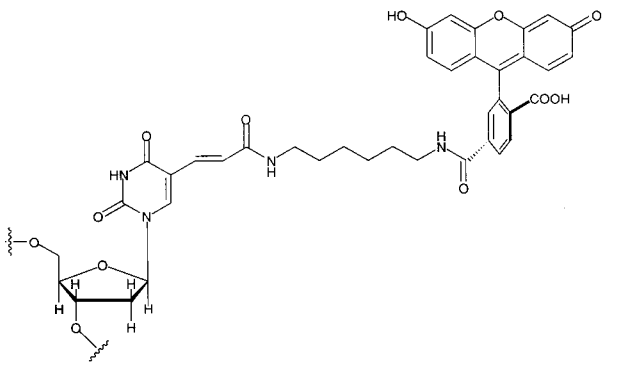

Probe A: 5′-CCT CU^{FL}C **TG*G*A** CCT TCC-3′
3′-GGA GA G AC C T GGA AGG-5′

Probe B: 5′-CCT CU^{FL}C **TG*G*T** CCT TCC-3′
3′-GGA GA G AC C A GGA AGG-5′

Probe C: 5′-CCT CU^{FL}C **TG*G*C** CCT TCC-3′
3′-GGA GA G AC C G GGA AGG-5′

Probe D: 5′-CCU^{FL} CTC **TG*G*A** CTC TCC-3′
3′-GGA GAG AC C T GAG AGG-5′

Probe E: 5′-CCT CU^{FL}C **TG*G*A** CTC TCC-3′
3′-GGA GA G AC C T GAG AGG-5′

Probe F: 5′-CCT CTC **TG*G*A** CU^{FL}C TCC-3′
3′-GGA GAG AC C T GA G AGG-5′

Probe G: 5′-CCT CTC **TG*G*A** CTC U^{FL}CC-3′
3′-GGA GAG AC C T GAG A GG-5′

FIGURE 1: Diagram of the fluorescein-modified deoxyuridine residue (fluorescein−dU) and platinated, fluorescent 16 bp DNA probes. The location of the fluorescein−dU moiety is denoted by U^{FL}, and the position of the cisplatin adduct is denoted by asterisks.

EXPERIMENTAL PROCEDURES

Materials and Methods. Distilled, deionized water from either a Milli-Q (Millipore) or a Nanopure (Barnstead) system was used to prepare all aqueous solutions. Atomic absorption spectrometry was performed on a Varian AA1475 instrument with a GTA-95 graphite furnace. High-performance liquid chromatography (HPLC) was carried out with a Waters system, which included a model 600E controller and a model 486 detector. A Branson sonifier 450 was used to lyse *Escherichia coli* cells for protein expression. Oligonucleotides were synthesized on an Applied Biosystems 392 DNA/RNA synthesizer. A Bio-Rad Econo liquid chromatography system and Amersham Pharmacia Biotech FPLC instrument were used for protein purification. Cerenkov radioactivity was measured in a Beckman 6500 liquid scintillation counter, and Kodak X-Omat film was used for autoradiography.

Expression and Purification of HMG-Domain Proteins. Expression and purification of HMG1 (*28*), HMG1 domains A and B (*13*), and the HMG1 domain A F37A mutant (*29*) were carried out as described.

Synthesis of a Platinated, Nonfluorescent 16 bp Duplex Probe. The synthesis and purification of the top (5′-CCT TCT TG*G*A CCT TCC-3′, where G* represents the site of platinum binding) and complementary bottom strands for a nonfluorescent 16 bp DNA duplex probe were carried out as described previously (*30*). Duplex DNA was prepared by combining equal amounts of top and bottom strands in 10 mM Tris (pH 7.0), 50 mM NaCl, and 10 mM $MgCl_2$, heating to 90 °C, and slowly cooling to 4 °C over several hours. The purity of the final duplex material was examined by analytical ion exchange HPLC.

Synthesis of Platinated, Fluorescent 16 bp DNA Probes. Figure 1 depicts the fluorescein-modified deoxyuridine (dU) residue and the DNA probes used in these studies. The positions of the cisplatin modification and fluorescein−dU are denoted in the sequences. The fluorescein-labeled top strands and complementary bottom strands were synthesized on a 1 μmol scale by using standard cyanoethylphosphoramidite chemistry with the coupling time for the fluorescein−dU (Glen Research) extended to 10 min. Following deprotection, the oligonucleotides were purified on 20% denaturing polyacrylamide gels.

An activated cisplatin solution was made by reaction with 1.97 molar equiv of $AgNO_3$ in distilled, deionized water with agitation at room temperature overnight in the dark followed by filtration through a 0.2 μm filter to remove the AgCl precipitate. A portion of each of the top strands was allowed to react with 1.2 equiv of the activated cisplatin solution in 10 mM sodium phosphate buffer (pH 6.8) for ~8 h at 37 °C. The platinated DNA was isolated by ethanol precipitation.

Double-stranded probes were prepared by combining equal amounts of top and bottom strands in 10 mM Tris (pH 7.0), 50 mM NaCl, and 10 mM $MgCl_2$, heating to 90 °C, and slowly cooling to 4 °C over several hours. The duplex DNA was purified by ion exchange HPLC using a Dionex Nucleopac PA-100 (9 mm × 250 mm) preparatory column at a flow rate of 4 mL/min. The DNA was eluted with a linear gradient of 70% buffer A (0.025 M NH_4OAc in 10% CH_3CN)/30% buffer B (buffer A and 1 M NaCl) to 45% buffer A/55% buffer B over the course of 30 min, followed by 45% buffer A/55% buffer B to 100% buffer B over the course of the next 10 min. Under these conditions, the duplexes eluted at ~23 min. The collected samples were desalted and reannealed in 10 mM Tris (pH 7.0), 50 mM NaCl, and 10 mM $MgCl_2$ by heating to 90 °C and slowly cooling to 4 °C over several hours. The purity of the final duplex material was examined by analytical ion exchange HPLC. The platinated 16-mer DNA strands were characterized by platinum atomic absorption spectroscopy and electrospray mass spectrometry (see Supporting Information, Tables S1 and S2).

Synthesis of a Platinated, Fluorescent 71 bp DNA Probe. Three oligonucleotides, a 37-mer, 18-mer, and 71-mer, were prepared on a 1 μmol scale by using standard cyanoethylphosphoramidite chemistry. Following deprotection, the oligonucleotides were purified by denaturing polyacrylamide gel electrophoresis. The synthesis of the platinated, fluorescent 16-mer (top strand, probe A, Figure 1) is described above. Supplied as Supporting Information (Figure S1) is a schematic diagram of the synthesis and purification of the fluorescent 71-mer DNA probe.

Equal amounts (25 nmol) of the 16-mer and 18-mer probes were phosphorylated on the 5′-ends in a reaction mixture containing 70 mM Tris-HCl (pH 7.6), 10 mM $MgCl_2$, 5 mM DTT, 12 mM ATP, and 1000 units of T4 polynucleotide kinase (New England Biolabs). The reaction mixture was incubated at 37 °C for 45 min, and then another 1000 unit aliquot of kinase was added. The reaction mixture was incubated at 37 °C for an additional 45 min and then extracted twice with one portion each of a 25:24:1 phenol/$CHCl_3$/isoamyl alcohol mixture followed by ethanol precipitation.

Double-stranded DNA probes were prepared by combining 5 nmol of 37-mer, 25 nmol of phosphorylated 16-mer, 25 nmol of phosphorylated 18-mer, and 5 nmol of 71-mer in 50 mM Tris (pH 7.9), 10 mM $MgCl_2$, 100 mM NaCl, and 1 mM DTT, heating to 90 °C, and slowly cooling to 4 °C over several hours. The annealed oligonucleotides were ligated in a reaction mixture containing 2.7 mM ATP, 0.06 μg/μL BSA, and 30 000 units of T4 DNA ligase (New England Biolabs) in 50 mM Tris (pH 7.9), 10 mM $MgCl_2$, 100 mM NaCl, and 1 mM DTT. The ligase reaction mixture was incubated at room temperature for 45 min followed by incubation for 16 h at 16 °C. The ligation reaction mixture was extracted twice with one portion each of a 25:24:1 phenol/$CHCl_3$/isoamyl alcohol mixture followed by ethanol precipitation. The precipitated DNA was further desalted by using a Centricon 10 apparatus (Millipore).

A small aliquot of the desalted DNA was radioactively labeled on the 5′-ends and run next to the unlabeled ligation reaction mixture on a 10% denaturing polyacrylamide sequencing gel for purification. The gel was visualized by autoradiography, and the film was used as a guide to excise the purified 71-mer DNA strands from the ligation reaction. The 71-mer strands were eluted from the gel by crush and soak methods and isolated by ethanol precipitation. The 71-mer strands were dissolved in 10 mM Tris (pH 7.0), 50 mM NaCl, and 10 mM $MgCl_2$, and annealed by heating to 90 °C, followed by slow cooling to 4 °C over several hours. A small aliquot of the annealed 71-mer was radioactively labeled on the 5′-ends and run next to the unlabeled, annealed 71-mer on a 15% native polyacrylamide gel for purification. The radioactive bands were visualized by autoradiography, and the film was used as a guide to excise the purified 71-mer DNA duplex. The 71-mer was eluted from the gel by crush and soak methods and isolated by ethanol precipitation.

Stopped-Flow Studies with Respect to the Kinetics of Protein−DNA Binding. Stopped-flow studies were performed by using a Hi-Tech SF-61 DX2 double-mixing stopped-flow apparatus. The excitation wavelength was 480 nm. Either a GG495 glass cutoff filter with a Wratten gel filter #58 (Kodak) or a 520 nm band-pass interference filter (Oriel) was placed over the exit to the photomultiplier tube to observe the fluorescein fluorescence emission. The platinated, fluorescent DNA probes described above were used at a final concentration of 25 or 50 nM in 10 mM HEPES (pH 7) and 200 mM NaCl. Pseudo-first-order kinetic conditions were maintained by using an at least 5-fold excess of protein in all experiments. Unless otherwise noted, experiments were performed at 4 °C.

Concentration-dependent studies were performed with the cisplatin-modified probes and HMG1 domains A and B to determine the rate constants for the binding and dissociation of the protein−DNA complexes. In these experiments, a fluorescent, platinated DNA probe was combined with a range of HMG-domain protein concentrations. Multiple shots were taken at each protein concentration. The observed rate constants for the protein concentrations were determined by fitting individual traces with the Kinet-Assyst software package (Hi-Tech) and averaging the results. The observed rate constant, k_{obs}, was plotted against the total protein concentration, $[P_t]$. The resulting linear plot is described by eq 1, where k_{on} is the second-order rate constant for protein binding and k_{off} is the first-order rate constant for the dissociation of the protein−DNA complex. The rate constants, determined by fitting the data to eq 1, were used to calculate a dissociation constant, K_d, for the protein−DNA complex according to eq 2.

$$k_{obs} = k_{on}[P_t] + k_{off} \quad (1)$$

$$K_d = k_{off}/k_{on} \quad (2)$$

Temperature-dependent studies were performed with some of the platinated DNA probes in Figure 1 and HMG1 domain A to reveal activation parameters for these protein−DNA complexes. Values for k_{on} and k_{off} over the temperature range of 4−20 °C were determined by performing concentration-dependent studies as described above at different temperatures. The activation enthalpy, $\Delta H^{\ddagger}$, and activation entropy, $\Delta S^{\ddagger}$, were determined from a plot of $R[\ln(k/T) - \ln(k_B/h)]$ against $1/T$ (eq 3), where R is the ideal gas constant, k is the rate constant (either k_{on} or k_{off}), k_B is the Boltzmann constant, h is Planck's constant, and T is the temperature (in kelvin).

$$R[\ln(k/T) - \ln(k_B/h)] = \Delta S^{\ddagger} - \Delta H^{\ddagger}\,(1/T) \quad (3)$$

Competition Stopped-Flow Kinetic Studies. Competition stopped-flow studies were performed by using a Hi-Tech SF-61 DX2 double-mixing stopped-flow apparatus. The excitation wavelength was 480 nm, and a 520 nm band-pass interference filter (Oriel) was placed over the exit to the photomultiplier tube to observe the fluorescein fluorescence emission.

Displacement kinetics experiments with HMG1 domain A were carried out by mixing a protein−DNA complex solution with an excess of platinated, competitor DNA. Over a temperature range of 4−20 °C, dissociation rate constants, k_{off}, were measured as the protein leaves the preformed complex and binds to the competitor DNA. Two protocols were adopted. In the first, a solution containing 50 nM probe A (Figure 1) and 50 nM HMG1 domain A in 10 mM HEPES (pH 7) and 200 mM NaCl was combined with a 500 nM solution of nonfluorescent, platinated, competitor DNA of the same sequence in the same buffer. The situation was reversed in the second set of experiments. Here a solution

of 50 nM nonfluorescent, platinated 16-mer and 50 nM HMG1 domain A in 10 mM HEPES (pH 7) and 200 mM NaCl was mixed with a 500 nM solution of probe A in the same buffer. Several shots were taken at each different temperature. Each trace was fit to a single-exponential equation by using the Kinet-Assyst software (Hi-Tech) to obtain the observed rate constant. The values were averaged to determine k_{off} for the protein−DNA complex at each temperature that was studied.

An additional set of competition experiments was performed to examine whether the fluorescent label inhibits protein binding. A solution of 50 nM probe A (Figure 1) in 10 mM HEPES (pH 7) and 200 mM NaCl was combined with 0.5 or 1 equiv of HMG1 domain A in the same buffer at 4 °C. The fluorescence change was monitored over time, and these results were compared to those obtained from mixing a solution of 25 nM probe A and 25 nM nonfluorescent, platinated 16-mer probe with the same concentrations of protein.

Finally, protein competition studies were performed with HMG1 domains A and B and the F37A domain A mutant protein at 4 °C. In these experiments, a solution of 50 nM probe E (Figure 1) and one of the three HMG-domain proteins (at 50 nM) in 10 mM HEPES (pH 7) and 200 mM NaCl was combined with one of the two remaining proteins (at 50 or 500 nM). The fluorescence change of the fluorescein in probe E was monitored over time to measure the effect of adding a competitor HMG-domain protein.

Modeling the Interaction of the Fluorescein with the HMG-Domain Proteins. The interaction of the fluorescein−dU with an HMG-domain protein was modeled by using the program Insight II (Molecular Simulations, Inc.). The PDB coordinates for the X-ray crystal structure of a platinated 16-mer duplex with HMG1 domain A (*29*) were loaded into Insight. The fluorescein moiety was built in Quanta 97 (Molecular Simulations, Inc.), minimized by using the CHARMm routine, imported into Insight II, and attached to the DNA from the X-ray structure at either the fifth or twelfth nucleotide of the platinated strand to create a fluorescein−dU. After the appropriate potentials had been set, the position of the fluorescein dye was minimized by using a Newton−Raphson conjugate gradient in the Discover module with the cvff. The positions of the DNA and protein from the crystal structure were fixed during the minimization.

RESULTS

DNA Probes with the Fluorescein−dU Moiety at Position T5

A Sequence-Dependent Study of HMG1 Domain A with 16 bp Probes. An example of the stopped-flow results from rapid mixing of HMG1 domain A with a platinated DNA probe having fluorescein−dU at T5 is given in Figure 2A. When the protein and DNA solutions were mixed, a large increase in fluorescein fluorescence intensity is observed. This change is not observed with fluorescently labeled oligonucleotides that do not contain a cisplatin adduct and is therefore attributed to a change associated with protein binding to platinated DNA. The stopped-flow data were fit to a single-exponential equation to obtain an observed rate constant, k_{obs}. Several such experiments were performed at

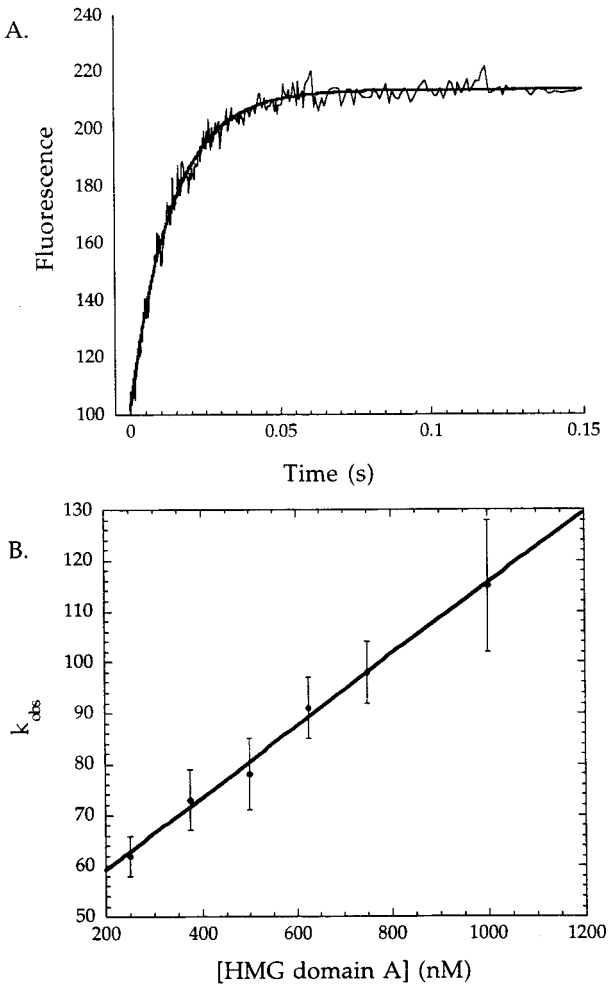

FIGURE 2: Stopped-flow results for HMG1 domain A binding to platinated 16-mer probes with a fluorescein−dU moiety at position T5. Panel A shows the fluorescence change that occurs upon mixing protein and DNA. Panel B plots the results of concentration-dependent studies in which eq 1 was used to determine binding and dissociation rate constants.

different protein concentrations and different temperatures. Average values for k_{obs} were obtained as described above and plotted against the protein concentration according to eq 1, affording the binding, k_{on}, and dissociation, k_{off}, rate constants for protein−DNA complexes with DNA probes A−C and E. An example of one such plot is given in Figure 2B. The k_{on} data obtained from these plots are listed in Table 1, and k_{off} values are reported in Table 2. Equation 2 was used to calculate dissociation constants, K_d, for these protein−DNA complexes. The results are given in Table 3. The kinetic and thermodynamic data in Tables 1−3 clearly demonstrate a dependence on the DNA sequence flanking the cisplatin adduct. Probes A and E, with a TGGA sequence, consistently have k_{on} values for HMG1 domain A binding that are 2−4 times larger than those determined for probes B and C with TGGT and TGGC sequences, respectively. The k_{off} values obtained for all the probes are more similar. Thus, k_{on} is the major contributor to differences observed in the K_d values calculated with eq 2.

Temperature-dependent studies allowed activation parameters to be determined. Figure 3 displays an example of a plot used to determine the activation parameters. In this analysis, $R[\ln(k/T) - \ln(k_B/h)]$ is plotted versus $1/T$, and the activation enthalpy and entropy were determined from the

Table 1: Binding Rate Constant, k_{on} (M^{-1} s^{-1}), Values for HMG1 Domain A and 16 bp Probes with the Fluorescein−dU Moiety at Position T5

temp (°C)	probe A	probe B	probe C	probe E
4	$(9 \pm 2) \times 10^7$	$(2.5 \pm 1) \times 10^7$	$(4 \pm 1) \times 10^7$	$(9 \pm 2) \times 10^7$
8	$(1.5 \pm 0.3) \times 10^8$	$(3.7 \pm 1.4) \times 10^7$	$(5 \pm 1) \times 10^7$	$(1.2 \pm 0.4) \times 10^8$
10	$(1.6 \pm 0.3) \times 10^8$	$(4.8 \pm 0.3) \times 10^7$	$(7.2 \pm 2) \times 10^7$	$(2.1 \pm 0.3) \times 10^8$
12	$(2.3 \pm 0.3) \times 10^8$	$(6.6 \pm 1.9) \times 10^7$	$(5.2 \pm 0.5) \times 10^7$	$(1.8 \pm 0.5) \times 10^8$
15	$(3 \pm 0.5) \times 10^8$	$(1.2 \pm 0.2) \times 10^8$	$(1.2 \pm 0.2) \times 10^8$	$(2.5 \pm 0.5) \times 10^8$
16	$(3 \pm 0.3) \times 10^8$	$(1.6 \pm 0.1) \times 10^8$	$(1.4 \pm 0.6) \times 10^8$	$(2.7 \pm 0.4) \times 10^8$
20	$(4.7 \pm 1.3) \times 10^8$	$(2.1 \pm 0.3) \times 10^8$	$(1.9 \pm 0.5) \times 10^8$	$(4.7 \pm 0.4) \times 10^8$

Table 2: Dissociation Rate Constant, k_{off} (s^{-1}), Values for HMG1 Domain A and 16 bp Probes with the Fluorescein−dU Moiety at Position T5

temp (°C)	probe A	probe B	probe C	probe E	fluorescent competitor[a]	nonfluorescent competitor[a]
4	30 ± 11	35 ± 4	26 ± 5	26 ± 5	27 ± 4	19 ± 1
8	34 ± 1	54 ± 8	44 ± 7	37 ± 8	38 ± 4	31 ± 2
10	64 ± 8	63 ± 2	72 ± 6	63 ± 13		
12	52 ± 16	73 ± 5	101 ± 16	61 ± 11	49 ± 11	44 ± 5
15	88 ± 18	86 ± 9	103 ± 7	117 ± 22		
16	88 ± 27	97 ± 4	123 ± 2	89 ± 5	49 ± 12	60 ± 10
20	130 ± 50	137 ± 14	197 ± 37	122 ± 28	153 ± 91	76 ± 9

[a] Probe A.

Table 3: Dissociation Constant, K_d, Values for HMG1 Domain A and 16 bp Probes with the Fluorescein−dU Moiety at Position T5

temp (°C)	probe A	probe B	probe C	probe E
4	333 ± 143 nM	1.4 ± 0.6 μM	650 ± 205 nM	289 ± 85 nM
8	227 ± 46 nM	1.4 ± 0.6 μM	880 ± 225 nM	308 ± 122 nM
10	400 ± 90 nM	1.3 ± 0.1 μM	1.0 ± 0.3 μM	300 ± 76 nM
12	226 ± 76 nM	1.1 ± 0.3 μM	1.9 ± 0.4 μM	339 ± 123 nM
15	293 ± 77 nM	717 ± 141 nM	858 ± 154 nM	468 ± 128 nM
16	293 ± 94 nM	606 ± 45 nM	878 ± 377 nM	330 ± 52 nM
20	277 ± 131 nM	652 ± 115 nM	1.0 ± 0.3 μM	260 ± 64 nM

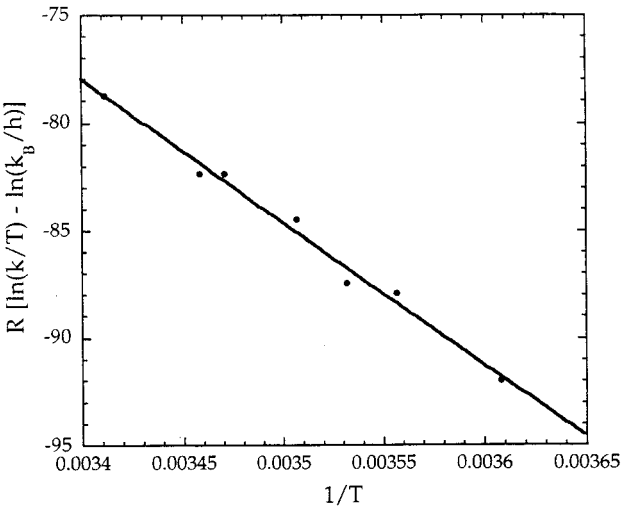

FIGURE 3: Example of data from temperature-dependent stopped-flow studies with HMG1 domain A. Activation parameters are determined from this plot according to eq 3.

slope and intercept on the ordinate according to eq 3. Activation parameters for DNA probes A−C and E are listed in Table 4. A dependence on the DNA sequence flanking the cisplatin adduct is also noted here, the activation parameters for the TGGA sequences varying somewhat from those of the TGGT and TGGC sequences.

Stopped-Flow Experiments with HMG1 Domain A and Competitor Oligonucleotides. Examples of the results from displacement kinetics experiments are given in Figure 4. Panel A displays the results of experiments performed with excess nonfluorescent, platinated competitor DNA. The fluorescence decreases over time as HMG1 domain A dissociates from probe A (Figure 1) and binds to the excess

Table 4: Activation Parameters for Binding and Dissociation of HMG1 Domain A with 16 bp Probes with the Fluorescein−dU Moiety at Position T5

	probe A	probe B	probe C	probe E
binding				
$\Delta H^{\ddagger}$ (kJ/mol)	66 ± 3	96 ± 7	68 ± 12	64 ± 7
$\Delta S^{\ddagger}$ (J K^{-1} mol^{-1})	148 ± 12	243 ± 26	144 ± 41	139 ± 26
dissociation				
$\Delta H^{\ddagger}$ (kJ/mol)	62 ± 8	53 ± 2	80 ± 8	67 ± 10
$\Delta S^{\ddagger}$ (J K^{-1} mol^{-1})	7 ± 29	−24 ± 8	76 ± 27	25 ± 34

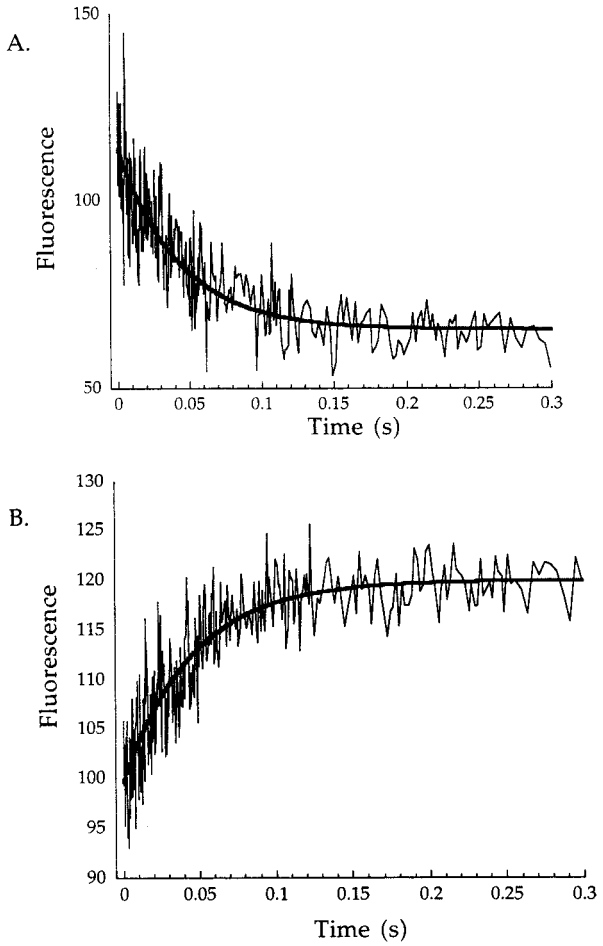

FIGURE 4: Data from displacement kinetics experiments. Panel A shows data from an experiment with nonfluorescent competitor DNA, and panel B displays the results from experiments with probe A as the competitor.

nonfluorescent DNA. Panel B shows data from the converse experiment with excess probe A. Here, the fluorescein fluorescence increases over time as the HMG1 domain A dissociates from the nonfluorescent DNA and binds to the excess probe A. Both sets of data were fit to a single-exponential equation to give an observed rate constant, k_{obs}. Under conditions where k_{on} is sufficiently large, these k_{obs} values are equivalent to k_{off}, because the rate-limiting step in the displacement is dissociation of the protein from the original protein−DNA complex. Thus, these experiments provide an independent measure of k_{off} values for the protein−DNA complex that can be compared with those determined through the concentration-dependent studies described above. These experiments were performed at several different temperatures, and the k_{off} values that were obtained are included in Table 2. The results are similar for both experimental procedures, indicating that the presence of the fluorescein−dU moiety does not significantly affect the binding of HMG1 domain A. The k_{off} values obtained in these studies are also in agreement with the results obtained from the concentration-dependent experiments.

Competition experiments were performed to examine whether the fluorescein−dU moiety affects protein binding. Solutions that were 50 nM in platinated DNA were combined with HMG1 domain A. In one set of experiments, the platinated DNA was 100% fluorescently labeled. The results were compared with data from experiments where only 50% of the DNA had a fluorescein−dU moiety (Figure S2). The 100% labeled DNA exhibited approximately twice the overall fluorescence change of the 50% labeled solution, as expected for the protein binding equally to both fluorescent and nonfluorescent DNA. The data demonstrate that the fluorescein−dU moiety does not adversely affect protein binding, a finding independently confirmed by gel mobility shift studies (Figure S3).

HMG1 Domain A with a 71-mer DNA Probe. The dependence of the length of the probe on the binding and dissociation kinetics of the protein−DNA complex was investigated by using a 71-mer fluorescent, platinated oligonucleotide with a TGGA sequence. When the protein and DNA solutions were mixed, a large fluorescein fluorescence increase was observed, just as with the 16 bp probes. The stopped-flow data were analyzed as described above to obtain the binding, k_{on}, and dissociation, k_{off}, rate constants for this protein−DNA complex at 4 °C. The second-order binding rate constant, k_{on}, was determined to be $(1.1 \pm 0.2) \times 10^8$ M^{-1} s^{-1}, and the first-order dissociation rate constant, k_{off}, was 31 ± 4 s^{-1}. The dissociation constant, K_d, for this protein−DNA complex was calculated to be 282 ± 63 nM using eq 2. These results are very similar to those obtained with the 16-mer oligonucleotides with a TGGA sequence (probes A and E, Figure 1), suggesting that the length of the oligonucleotide does not affect the kinetics of protein−DNA complex formation. An example of the stopped-flow data obtained at 4 °C with this oligonucleotide and HMG1 domain A is presented in Figure S4.

Stopped-Flow Studies with a F37A HMG1 Domain A Mutant. A recent X-ray crystal structure determination of HMG1 domain A bound to a 16 bp cisplatin-modified oligonucleotide revealed that phenylalanine 37 (F37) of the HMG-domain intercalates into a hydrophobic notch created by a platinum atom binding to the N7 positions of two adjacent guanine bases (*29*). Gel mobility shift assays with a mutant HMG1 domain A, where the phenylalanine was changed to an alanine residue (F37A), demonstrated that F37 was important for binding. In those studies, the binding affinity of the F37A mutant was significantly reduced (*29*). Stopped-flow studies were performed here with the F37A domain A mutant and probe A (Figure S5). The fluorescence change for the F37A mutant was largely extinguished compared to that obtained with the wild-type protein, indicating that protein binding to the DNA, while not totally abolished, is significantly diminished. The observed rate constant values with the F37A mutant were somewhat larger than with HMG1 domain A. For example, k_{obs} was 86 ± 13 s^{-1} at 350 nM F37A, compared to a k_{obs} of 55 ± 2 s^{-1} with 368 nM HMG1 domain A.

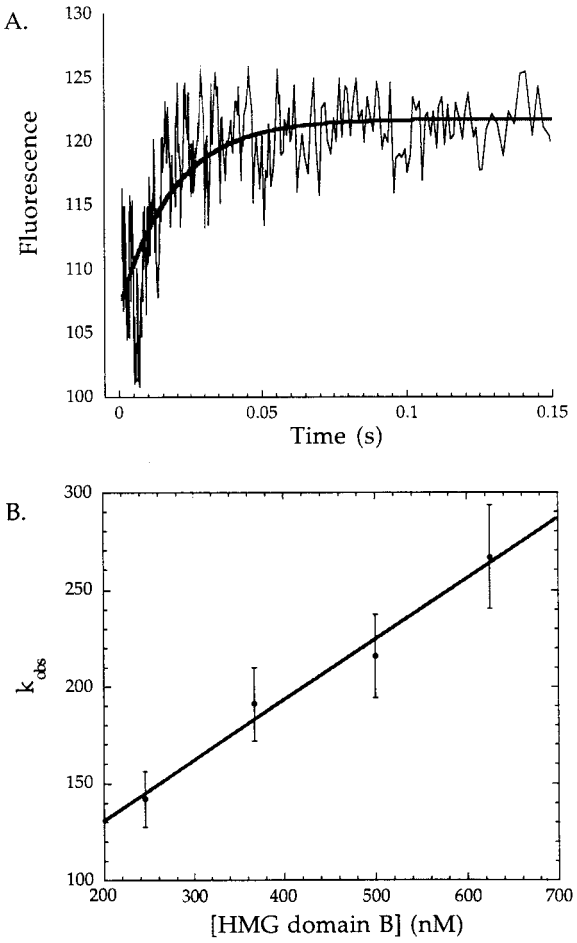

FIGURE 5: Stopped-flow results for HMG1 domain B binding to platinated 16-mer probes with a fluorescein−dU moiety at position T5. Panel A shows the fluorescence change that occurs upon mixing protein and DNA. Panel B plots the results of concentration-dependent studies in which eq 1 was used to determine binding and dissociation rate constants.

HMG1 Domain B with 16 bp Probes. An example of the stopped-flow results from an average of several shots of HMG1 domain B binding to a platinated, fluorescent DNA probe with the fluorescein−dU moiety at T5 at 4 °C is given in Figure 5A. As with the F37A domain A mutant, there is only a small fluorescein fluorescence change, indicating that the binding of HMG1 domain B differs somehow from that of HMG1 domain A. Despite the small magnitude of the fluorescence change, the stopped-flow data could be fit to a single-exponential equation to obtain an observed rate

Table 5: Rate and Dissociation Constant Data for HMG1 Domain B and 16 bp Probes with the Fluorescein−dU Moiety at Position T5

oligonucleotide	k_{on} (M^{-1} s^{-1})	k_{off} (s^{-1})	K_d (nM)
probe A	$(1.9 \pm 1.3) \times 10^8$	86 ± 56	453 ± 428
probe B	$(2.4 \pm 1.5) \times 10^8$	73 ± 34	304 ± 237
probe C	$(2.7 \pm 1.5) \times 10^8$	77 ± 50	285 ± 244
probe E	$(2.2 \pm 1) \times 10^8$	134 ± 72	609 ± 430

constant, k_{obs}. Several shots were taken at different protein concentrations, and average values for k_{obs} were obtained as described above. These average k_{obs} values were plotted against the protein concentration, according to eq 1, to calculate the binding, k_{on}, and dissociation, k_{off}, rate constants for protein−DNA complexes at 4 °C with DNA Probes A−C and E. An example of one of these plots is given in Figure 5B. The k_{on}, k_{off}, and K_d values for these protein−DNA complexes are listed in Table 5. For the TGGA sequences, the k_{on} values are similar for HMG1 domains A and B, but the k_{off} values are larger with HMG1 domain B. Unlike the results with HMG1 domain A, there is no clear dependence of k_{on} on the DNA sequence flanking the cisplatin−DNA adduct. Hence, the k_{on} values for the TGGT and TGGC sequences are significantly larger with HMG1 domain B than with HMG1 domain A.

Stopped-Flow Studies with HMG1. The fluorescence intensity changes observed here in stopped-flow experiments for the two individual HMG domains from HMG1 are significantly different. We were therefore interested in examining the results obtained with the full-length HMG1 protein, where domains A and B are both present in tandem. A comparison of stopped-flow data for HMG1 domain A and the full-length HMG1 protein binding to probe E revealed the overall fluorescein fluorescence intensity change to be similar for both proteins (Figure S6). These results suggest that domain A may ultimately control binding of the full-length protein. The kinetic behavior of these two proteins, however, is distinctly different. The trace for HMG1 domain A is best described by a single exponential, whereas the data for HMG1 are clearly multiexponential. This result may be due to a more complex binding interaction occurring in the full-length protein, where both HMG domains could be participating.

Protein Competition Stopped-Flow Experiments. Differences in the binding of the HMG domains were further highlighted through protein competition stopped-flow studies (Figure S7). In these experiments, a preformed complex of probe E and HMG1 domain A was allowed to react with HMG1 domain B or the F37A domain A mutant. When 1 or 10 equiv of either protein was mixed, there was only a small decrease in the fluorescence intensity over time. This result could be due to a small amount of HMG1 domain A being replaced by HMG1 domain B or the F37A mutant. The observed rate constants in all of these experiments ranged from ~30 to 40 s^{-1}.

A different result was obtained upon mixing a preformed complex of probe E and HMG1 domain B or the F37A mutant with HMG1 domain A. In this case, a large fluorescence increase occurred that varied with the amount of HMG1 domain A. The observed rate constant of $\sim 25 \pm 1$ s^{-1} with 1 equiv of domain A increased to $\sim 39 \pm 1$ s^{-1} with 10 equiv of protein. The large fluorescence increase is probably due to HMG1 domain A replacing domain B or the F37A mutant in the initial protein−DNA complex. Only a very slight fluorescence change occurred when a preformed domain B complex was mixed with the F37A mutant or when a preformed F37A complex was mixed with domain B.

DNA Probes with the Fluorescein−dU Moiety at Position T3, T12, or T14

Up until this point, all the stopped-flow fluorescence results were obtained with the fluorescein−dU base at position T5, three bases to the 5′-side of the cisplatin cross-link. To observe what effect the position of the fluorescein−dU moiety might have on the fluorescence signal, additional stopped-flow studies were performed with probes D, F, and G (Figure 1). No fluorescence signal change occurred upon mixing HMG1 domain A or B with probes D and G. In these oligonucleotides, the fluorescein−dU moiety is positioned two bases away from the ends of the duplex, sites T3 and T14, respectively. In addition, the fluorescein fluorescence did not change when HMG1 domain B was combined with probe F, in which the fluorescein−dU moiety is placed three bases to the 3′-side of the cisplatin cross-link, T12. The overall fluorescence change observed when probe F was combined with HMG1 domain A was significantly diminished compared to those of probes having the fluorescein−dU moiety at T5 (Figure S8). The data were fit to a double-exponential equation to obtain two observed rate constants. Only the first, larger rate constant varied with protein concentration. Several shots were taken at different protein concentrations, and average values for the first rate constant were obtained. These average k_{obs} values were plotted against the protein concentration, according to eq 1, to calculate the binding, k_{on}, and dissociation, k_{off}, rate constants for this protein−DNA complex at 4 °C. The second-order rate constant for binding, k_{on}, was determined to be $(5.5 \pm 2) \times 10^8$ M^{-1} s^{-1}, and the first-order dissociation rate constant, k_{off}, was 103 ± 30 s^{-1}. The dissociation constant, K_d, for this protein−DNA complex was calculated to be 187 ± 87 nM using eq 2. These k_{on} and k_{off} values are several-fold larger than those obtained with the fluorescein−dU moiety at T5. Taken together, the results presented above clearly demonstrate that the interaction of the HMG-domain proteins with the fluorescein−dU moiety depends on the position of the fluorescent probe.

DISCUSSION

Fluorescence Change of the Fluorescein−dU Moiety upon HMG-Domain Protein Binding to Cisplatin-Modified DNA. A large, dramatic fluorescence change is observed in the stopped-flow experiments with the fluorescein−dU probe placed at the T5 position of a 16 bp cisplatin-modified duplex upon binding HMG1 domain A. A similar fluorescence increase was observed upon binding of UvrA and UvrB proteins to a tetramethylrhodamine−dU DNA probe (*27*). This effect is diminished in experiments performed with HMG1 domain B and depends on the position of the fluorescein−dU moiety. All of the stopped-flow data obtained with the fluorescein−dU probes follow pseudo-first-order kinetics in the presence of excess HMG domain and exhibit the expected linear dependence on protein concentration. In addition, the kinetic studies with HMG1 domain A

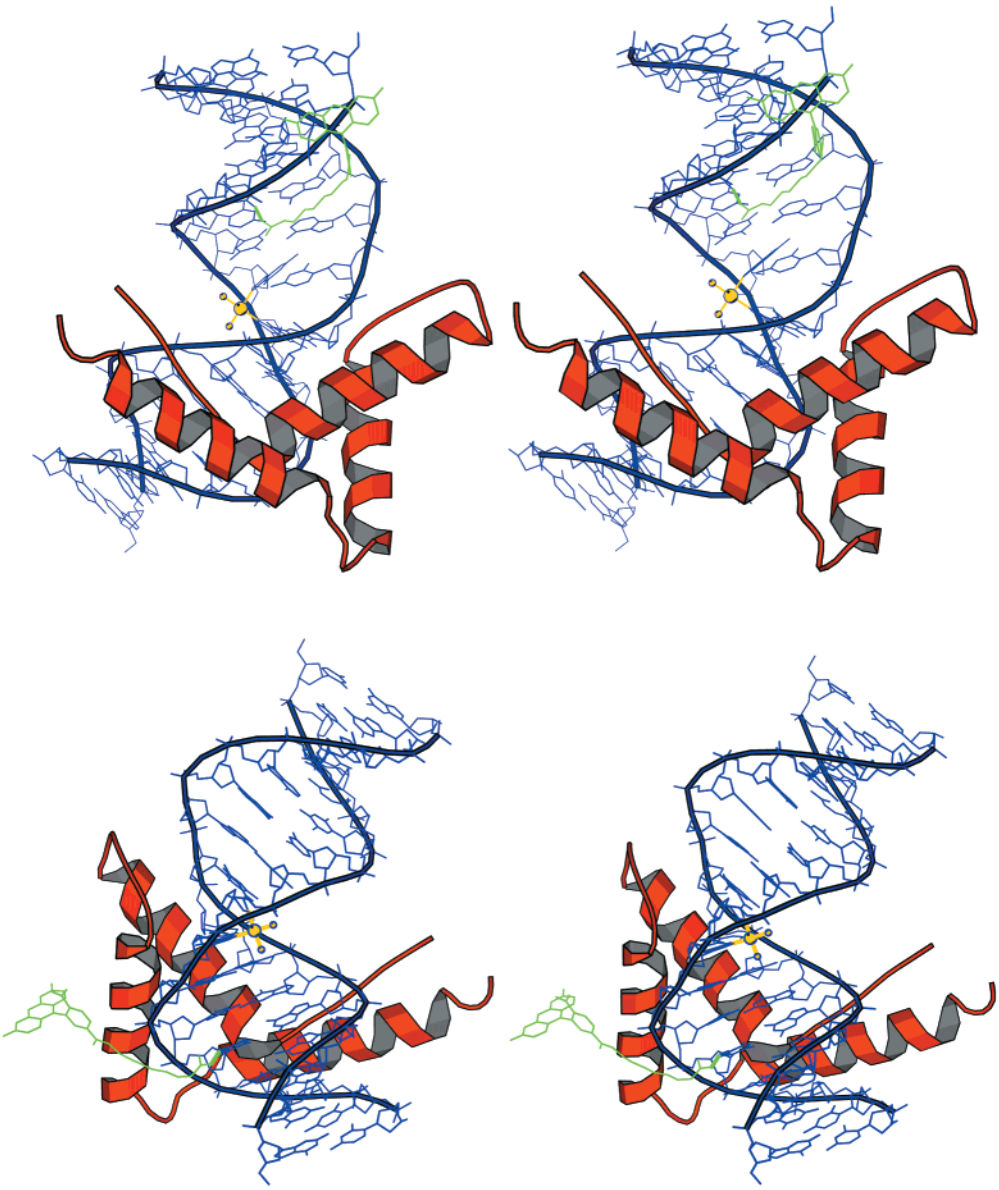

FIGURE 6: Stereoview of models of fluorescein−dU DNA probes drawn with MOLSCRIPT (*51*). DNA is depicted in blue, and the HMG domain is in red. The fluorescein is in green, and the $[Pt(NH_3)_2]^{2+}$ moiety is in yellow. The upper model is for the fluorescein−dU moiety at position T5, and the lower model has the fluorescein−dU moiety at position T12.

exhibit a dependence on the DNA flanking sequence context of the cisplatin cross-link that agrees with data from gel mobility shift assay studies (*13*). Thus, the results suggest that the fluorescence change is related to a protein binding event, the magnitude of which depends on the position of the fluorescent probe and the nature of the HMG-domain protein.

Molecular modeling studies were performed to examine the differences when the fluorescein−dU moiety was placed at residue T5, where the largest change occurred, compared to T12 in a complex with HMG1 domain A. The final minimized structures for these models are presented in Figure 6. In both cases, the fluorescein is initially in a position where it has the potential to interact with the HMG domain. After minimization, the fluorescein at T5 is located along the sugar−phosphate backbone pointing toward the 5′-end of the platinated strand. In contrast, in the minimized T12 structure, the fluorescein wraps around the DNA to interact more directly with the protein in the minor groove. These simple modeling studies demonstrate that the environment of the fluorescein dye clearly differs at these two positions. The asymmetry of domain A binding causes there to be more protein−DNA contacts in the vicinity of T12 (*29*), which may be responsible for the positioning of the fluorescein in the minimization. Thus, differences in the potential to interact with the HMG domain at these two positions, illustrated by these modeling studies, most likely underlie the different experimentally observed fluorescein fluorescence results.

The fluorescein−dU probe employed in this work is similar to a dansyl−dU probe used to examine local polarity in the major groove of DNA (*31*). In both cases, the fluorophore is linked to the C5 position of a deoxyuridine base, positioning it in the major groove of the DNA. Differences in fluorescence intensity were observed with different placements of the dansyl−dU probe (*25*, *26*), as occurred in the stopped-flow studies presented here. In fact, the results of the studies with the dansyl−dU probe showed the local polarity of the major groove to be sequence-dependent. Fluorescein is an environment-sensitive probe with a marked pH dependence (*32*−*34*). Therefore, it is

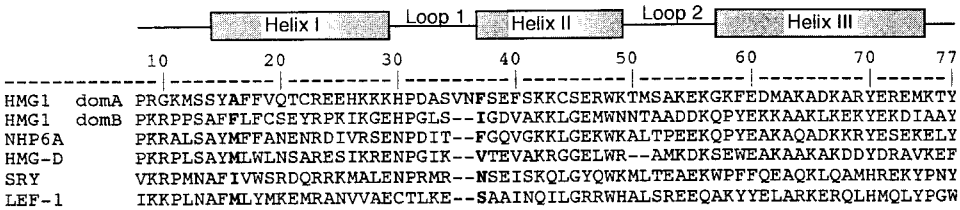

FIGURE 7: Sequence alignment of selected HMG domains. Positions 16 and 37 in the HMG1 domain A numbering scheme are in boldface type.

possible that the variations in fluorescence intensity observed with the fluorescein−dU probe are due to differences in the environment of the major groove at the T5 and T12 positions.

In addition to varying with the position of the fluorescein−dU moiety, the fluorescence intensity change also depends on the choice of HMG-domain protein. Only with HMG1 domain A is a large fluorescein fluorescence change observed. HMG1 domain B and the F37A domain A mutant produce more modest fluorescence changes. Some insight into these differences may be gained by examining the results from structural and modeling studies of DNA complexes of structure-specific HMG-domain proteins, such as HMG1 domain A, HMG-D, and NHP6A (*29*, *35*−*37*).

An X-ray crystal structure of HMG-D binding to linear DNA displays a smooth DNA bend over several base pairs accompanied by a widening of the minor groove (*36*). In this protein−DNA complex, the bend locus is near the center of the protein binding site, similar to the situation found for sequence-specific HMG-domain proteins such as LEF-1 and SRY (*38*, *39*). Other structure-specific HMG-domain proteins adopt a different conformation when binding to distorted, prebent DNA targets, however. Studies with cisplatin-modified DNA (*29*) and DNA containing a dA_2 bulge (*35*) show that the DNA bends sharply at the site of modification and the HMG-domain protein binds asymmetrically on one side of the bend. Structure-specific HMG-domain proteins, with the exception of HMG1 domain A, have hydrophobic residues near the start of helix I, position 16 in the HMG1 domain A numbering scheme (*29*), that can partially intercalate into the DNA (Figure 7). In addition, these proteins have a second set of intercalating residues at the amino terminus of helix II, position 37. Differences in the identity of these intercalating residues have been suggested to contribute to the different DNA binding activities of HMG-domain proteins (*29*, *36*) and may be relevant to the fluorescence changes observed in the stopped-flow studies presented here.

In the X-ray crystal structure of HMG1 domain A bound to a 16 bp cisplatin-modified oligonucleotide probe (*29*), a phenylalanine residue is intercalated into the hydrophobic notch created by the cisplatin-modified guanine rings. The ability of domain A to effect the large fluorescence change observed here might be due to the intercalation of this phenylalanine residue. HMG1 domain B has an isoleucine at the equivalent position, and the F37A domain A mutant has this phenylalanine mutated to an alanine. Neither residue has the ability to provide a stacking interaction with the guanine rings that has been suggested to be important in the binding of HMG1 domain A (*29*). Consequently, these proteins could bind in a different manner and not perturb the fluorescein−dU environment to the same extent. Thus, it may be that the presence of the intercalating phenylalanine in HMG1 domain A induces a distinct positioning of the protein, causing a unique interaction with the fluorescein−dU moiety and a large fluorescence change.

An alternative explanation for the fluorescence change is that, instead of a direct interaction with the protein residues, the environment of the fluorophore is perturbed through local structural changes caused by protein binding in the minor groove of the DNA. The dansyl−dU probe discussed above was used to examine the binding of the antitumor antibiotic, netropsin, to a DNA dodecamer (*25*, *26*). The presence of the dansyl−dU moiety in the major groove does not appear to affect the binding of netropsin in the minor groove (*25*, *26*). This result contrasts with data from experiments using the fluorescent base analogue, 2-aminopurine, where the amino group partially blocks the minor groove binding site (*40*, *41*). Similarly, the results of the stopped-flow studies with the competitor oligonucleotides and the gel mobility shift assays presented here demonstrate that the presence of the fluorescein−dU moiety does not affect the binding of HMG-domain proteins to any great extent.

The binding of netropsin widens the minor groove and bends the helix axis, without unwinding DNA (*42*). In addition, the spine of hydration in the minor groove is disrupted at the binding site (*43*, *44*). Many of these changes are similar to the effects observed when an HMG-domain protein binds (*29*). The dansyl−dU moiety exhibits an increase in fluorescence upon the binding of netropsin that is attributed to the results of local minor groove structural changes (*25*, *26*). A similar effect could be occurring in the stopped-flow studies here because the structural changes in the minor groove are comparable. The ability of HMG-domain proteins to bind in different manners, discussed above, could affect structural changes in the minor groove and consequently change the fluorescence intensity of the fluorescein−dU moiety.

Kinetic Parameters and Their Implications. The results of kinetic studies performed with HMG1 domain A exhibit a strong dependence on DNA sequence context at the cisplatin cross-link. There is good agreement with data from gel mobility shift assays where sequence context modulated the dissociation constant value by orders of magnitude (*13*). The flanking base on the 3′-side of the cisplatin adduct has the largest influence on complex stability, with the strongest binding occurring with dA followed by T and dC (*13*). Dissociation constants obtained from the stopped-flow data (Table 3) follow this trend. The differences in K_d depend entirely on k_{on}, the k_{off} values being similar for all the sequences. An interesting observation is that an alteration in DNA sequence at the third and fourth bases to the 3′-side of the cisplatin-adduct does not appear to affect the binding of HMG1 domain A. The sequence was altered by switching pyrimidine bases in probes A and E, and it would be

interesting to observe what effect would arise if a pyrimidine base were exchanged with a purine.

Overall, the binding of HMG1 domain A is fast, with k_{on} values nearing the diffusion limit. Dissociation of the protein also occurs relatively quickly. The half-life for the protein−DNA complex, calculated from the k_{off} values, is ∼20 ms at 4 °C and ∼5 ms at 20 °C. The length of the oligonucleotide does not affect the rate of binding or dissociation, since the rate constants obtained for a 71-mer DNA probe are essentially the same as those measured for a 16 bp probe with the same flanking DNA sequence. Because of this observation, it is unlikely that a "sliding" mechanism, where the protein diffuses along the DNA molecule, is occurring here. Such a process exhibits a characteristic dependence on the length of the DNA molecule (*45*). The quality of the stopped-flow data with HMG1 domain A allowed temperature-dependent studies to be performed to determine activation parameters. Similar values were obtained for both the binding and dissociation activation enthalpies, $\Delta H^{\ddagger}$, which explains why, within error, the K_d values are invariant with temperature. The activation entropies, $\Delta S^{\ddagger}$, for the binding event are larger than for dissociation of the protein from the DNA. This result can be rationalized by considering that counterions and ordered water molecules will be released at the protein−DNA interface, causing an increase in entropy upon their dissociation.

The fluorescence signal change obtained with HMG1 domain B was significantly diminished compared to that for HMG1 domain A. The lower signal-to-noise ratio afforded lower-quality data and did not allow studies to be performed above 4 °C. Nonetheless, as with HMG1 domain A, the binding of HMG1 domain B is fast with the k_{on} values nearing the diffusion limit. In fact, the rate constants for HMG1 domain B are all either the same as or larger than those obtained for HMG1 domain A. The sequence of the bases flanking the cisplatin cross-link did not influence the kinetic data with domain B, consistent with the results of gel mobility shift studies where the flanking nucleotide preference was much less pronounced with HMG1 domain B than with domain A (*13*). The dissociation of this protein−DNA complex is almost 3 times faster than with HMG1 domain A, with a half-life of ∼7 ms at 4 °C.

The kinetic data obtained here provide some insight into the different DNA binding properties of HMG1 domains A and B. Data collected with probes A and E (TGGA central sequence) demonstrate that both proteins have similar binding rate constants. The dissociation rate constants for HMG1 domain B are ∼3−4 times larger than those obtained with domain A, however. Thus, it is the off rate that is responsible for the larger dissociation constant. This binding affinity difference between domains was highlighted in the protein competition stopped-flow studies. Excess domain B could not effectively displace the prebound domain A protein, but excess domain A could displace the prebound domain B protein. The overall fluorescence change in studies with the full-length HMG1 protein indicates that it is domain A that controls the binding when both domains are present. These results are consistent with a recent footprinting study, where domain A mediated the structure-specific binding of an HMG1 AB didomain to four-way junction DNA (*46*).

Comparison with Rate Information from Other Kinetic Studies. The results of these experiments provide important information about the kinetics of HMG-domain proteins binding to cisplatin-modified DNA. Very little kinetic information is available for HMG-domain proteins binding to DNA in general. Data obtained through competition kinetic gel shift experiments revealed a dissociation rate constant of 1.1×10^{-4} s^{-1} for LEF-1 binding to its target DNA sequence (*47*). From the K_d of 1 nM determined in that work, the binding rate constant is calculated to be 1.1×10^5 M^{-1} s^{-1}. Surface plasmon resonance techniques were used to measure the binding of HMG1 and HMG2 to a 30 bp oligonucleotide (*48*). The k_{on} and k_{off} values for both of these proteins were $\sim 2 \times 10^4$ M^{-1} s^{-1} and $\sim 6-7 \times 10^{-2}$ s^{-1}, respectively. These results demonstrate that the binding and dissociation of LEF-1, HMG1, and HMG2 protein−DNA complexes with unmodified DNA occur much more slowly than for complexes with HMG1 domains A and B and cisplatin-modified DNA.

Kinetic parameters for HMG-domain proteins binding to cisplatin-modified DNA have been determined more directly through stopped-flow FRET studies (*18*). In these experiments, a 20 bp cisplatin-modified DNA probe was labeled at one end with a donor and at the other end with an acceptor dye. Distance changes between the donor and acceptor, caused by protein binding and bending of the DNA, were monitored via fluorescence intensity changes. The associative rate constants for HMG1 domains A and B binding to a cisplatin-modified probe at 4 °C in these FRET studies were $(1.0 \pm 0.3) \times 10^9$ and $(1.1 \pm 0.1) \times 10^9$ M^{-1} s^{-1}, respectively. These values are about 10-fold larger than those determined here with the fluorescein−dU probes. The k_{off} values measured for domains A and B were 52 ± 32 and 30 ± 4 s^{-1}, respectively, similar to those determined here.

One explanation for the differences in the k_{on} values obtained in the FRET stopped-flow studies and the values reported here is that the two types of fluorescent DNA probes may monitor two different phases of the binding event. A possible scenario is that initial binding of the protein induces a DNA bend. The protein is subsequently locked into place by intercalation of protein residues, producing a further conformational change. DNA probes used in the FRET study would respond to the DNA bend produced in the initial binding event. Any subsequent conformational changes would not be detected if the distance between the ends of the oligonucleotide remained unaltered. The fluorescence change of the fluorescein−dU moiety, on the other hand, may not be responsive to the initial binding event, but should detect subsequent conformational changes due to intercalation. The conformational change would depend on the position and degree of intercalation, explaining why the fluorescence change is diminished for the F37A domain A mutant and HMG1 domain B compared to HMG1 domain A. A similar two-step mechanism has been proposed for the TATA binding protein, which intercalates phenylalanine residues from the minor groove (*24*).

It would be interesting to compare the rate constants obtained from the stopped-flow experiments with the fluorescein−dU moiety to those from stopped-flow anisotropy experiments. Such studies should reveal a decrease in the rotational correlation time due to initial protein binding that would be detected as an anisotropy change. By comparing the rate constants from the anisotropy experiments with those

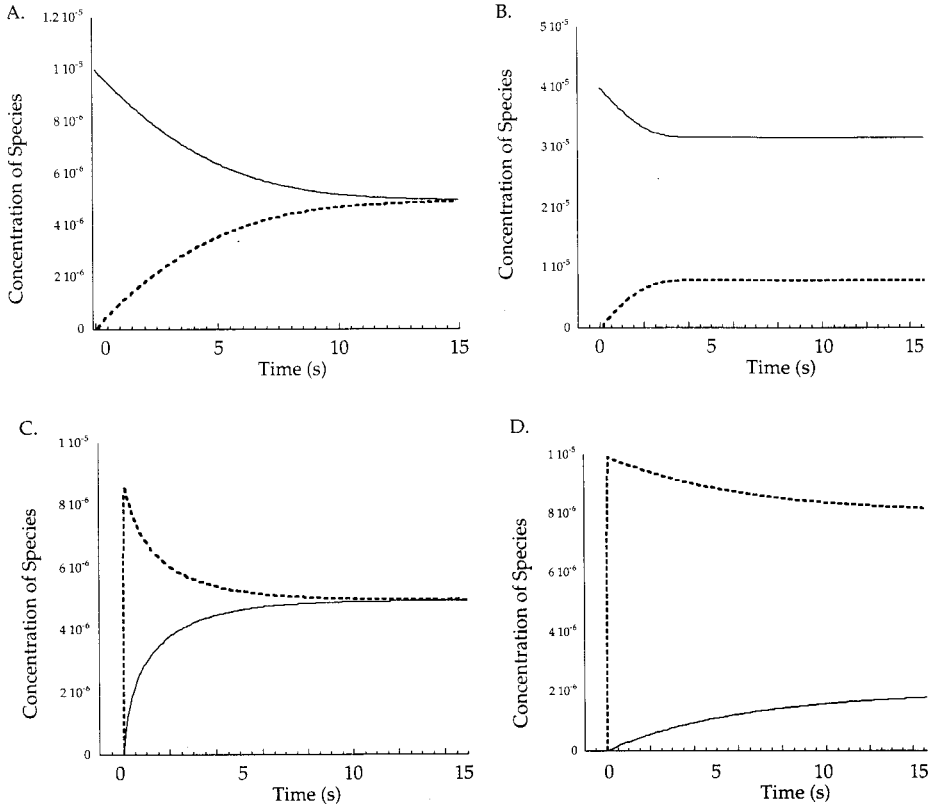

FIGURE 8: Kinetic simulation of the hijacking (A and B) and repair shielding (C and D) models. The forward and reverse rate constants for forming the HMG−Pt−DNA complexes (dashed lines) were set to 5×10^8 M^{-1} s^{-1} and 50 s^{-1}, respectively. The forward and reverse rate constants for forming the HMG−target DNA and repair−Pt−DNA complexes (solid lines) were set to 1×10^6 M^{-1} s^{-1} and 0.1 s^{-1}, respectively. In panel A, the initial concentrations of the HMG−target DNA complex and Pt−DNA were set to 10 μM. In panel B, the initial concentration of the HMG−target DNA complex was set to 40 μM and the concentration of Pt−DNA was set to 10 μM. In panel C, the initial concentrations of repair protein, HMG protein, and Pt−DNA were set to 10 μM. In panel D, the initial concentrations of repair protein and Pt-DNA were set to 10 μM, and the concentration of HMG protein was 40 μM.

obtained from fluorescence intensity changes, one could determine whether the two-step model presented here is feasible. Nonetheless, the data from both the FRET and present studies have determined a relatively narrow range for the binding and dissociation rate constants for complexes between HMG-domain proteins and cisplatin-modified DNA.

Implications for the Mechanism of Action of Cisplatin. Examining the kinetics of HMG-domain protein binding to cisplatin-modified DNA provides important fundamental information about the resulting complexes. The data are potentially valuable for understanding what role these proteins might play in sensitizing cells to this anticancer drug. One proposed mechanism of action for cisplatin has HMG-domain proteins diverted from their natural DNA binding sites to cisplatin−DNA adducts (*2*). The subsequent inability of such proteins to perform their normal functions contributes to cell death. Another proposal is that HMG-domain proteins shield cisplatin−DNA adducts from damage recognition proteins involved in nucleotide excision repair, and the persistence of the cisplatin cross-links on the DNA causes cell death (*2*). The kinetics of protein−DNA complex formation and dissociation are important in both of these leading hypotheses.

Competition between various protein−DNA complexes is important to both the hijacking and repair shielding mechanisms, as highlighted by an experiment that examined the interactions of RPA, a protein involved in DNA damage recognition in the nucleotide excision repair pathway, and HMG1 with cisplatin-modified DNA (*49*). The results revealed that, when both proteins were present, HMG1 selectively bound the platinated DNA at the expense of RPA complex formation. One possible explanation for this result is that the competition is kinetically controlled, and HMG1 binding to cisplatin-modified DNA occurs at a rate that is faster than the rate of RPA binding (*49*). The k_{on} values for domains A and B of HMG1 determined here are consistent with such an explanation, since they approach the diffusion limit.

Kinetics simulations performed with the program HopKINSIM, shown in Figure 8, demonstrate that HMG-domain proteins can compete in mechanisms such as those presented above. In these models, rate constants for complexes between HMG-domain proteins and platinated DNA were based on those determined experimentally. A model for the hijacking mechanism, where an HMG-domain protein can bind competitively to both its natural target and platinated DNA, is presented in panels A and B of Figure 8. In these simulations, the HMG-domain protein is initially bound to the natural target site. Over time, some of the HMG-domain protein is diverted to the platinated DNA, showing this model to be feasible for both concentrations of HMG-domain protein that were examined. The repair shielding model is presented in panels C and D. Here, repair and HMG-domain proteins compete for the platinated DNA target. Under all of the conditions that were examined, HMG-domain protein-platinated DNA complexes dominate at early time points.

With 1 equiv of HMG-domain protein (panel C), the levels of the platinated DNA complex eventually are diminished and level out as the repair complexes are formed; however, with excess HMG-domain protein (panel D), the platinated DNA complexes dominate over the repair complexes.

The availability of kinetic data obtained from studies such as those presented here allows modeling studies to be performed in an effort to examine the hijacking and repair shielding models. It is not known exactly what levels of HMG-domain protein-platinated DNA complexes would be necessary to produce a cytotoxic response in vivo. Moreover, we recognize that the parameters for HmG domains could differ from those of the full-length proteins. These simulations demonstrate, however, that complexes between HMG-domain proteins and platinated DNA can form at significant levels and potentially interfere with cellular processes through both of these proposed mechanisms. For example, a 2-fold elevation in the level of HMG1 in human, MCF-7 breast cancer cells effected by treatment with estrogen or progesterone is accompanied by a 2-fold sensitization of these cells to cisplatin (*50*). This result is consistent with a repair shielding mechanism.

ACKNOWLEDGMENT

We thank George Gassner and Daniel Kopp for help with the stopped-flow experiments, Seth Cohen for providing the nonfluorescent, cisplatin-modified 16-mer probe, Qing He for assistance with gel mobility shift studies, and Johnson Matthey for a gift of cisplatin.

SUPPORTING INFORMATION AVAILABLE

Electrospray mass spectrometry data (Table S1) and measured platinum levels (Table S2) of oligonucleotides used in this study; a schematic diagram of the synthesis and purification of the 71-mer DNA probe and kinetic data obtained with this probe (Figures S1 and S4, respectively); competition kinetic studies with 100% and 50% fluorescently labeled DNA (Figure S2); gel mobility shift assays with fluorescent and nonfluorescent DNA probes (Figure S3); results of stopped-flow studies with the F37A domain A mutant and HMG1 (Figures S5 and S6, respectively); data from the protein competition experiments (Figure S7); and the stopped-flow results with HMG1 domain A and a DNA probe with the fluorescein label at position T12 (Figure S8). This material is available free of charge via the Internet at http://pubs.acs.org.

REFERENCES

1. Zamble, D. B., and Lippard, S. J. (1999) in *Cisplatin: Chemistry and Biochemistry of a Leading Anticancer Drug* (Lippert, B., Ed.) pp 73−110, Verlag Helvetica Chimica Acta, Zurich.
2. Jamieson, E. R., and Lippard, S. J. (1999) *Chem. Rev. 99*, 2467−2498.
3. Loehrer, P. J., and Einhorn, L. H. (1984) *Ann. Intern. Med. 100*, 704−713.
4. Morris, M., Eifel, P. J., Lu, J., Grigsby, P. W., Levenback, C., Stevens, R. E., Rotman, M., Gershenson, D. M., and Mutch, D. G. (1999) *N. Engl. J. Med. 340*, 1137−1143.
5. Fichtinger-Schepman, A. M. J., van der Veer, J. L., den Hartog, J. H. J., Lohman, P. H. M., and Reedijk, J. (1985) *Biochemistry 24*, 707−713.
6. Grosschedl, R., Giese, K., and Pagel, J. (1994) *Trends Genet. 10*, 94−100.
7. Huang, J.-C., Zamble, D. B., Reardon, J. T., Lippard, S. J., and Sancar, A. (1994) *Proc. Natl. Acad. Sci. U.S.A. 91*, 10394−10398.
8. Zamble, D. B., Mu, D., Reardon, J. T., Sancar, A., and Lippard, S. J. (1996) *Biochemistry 35*, 10004−10013.
9. Brown, S. J., Kellett, P. J., and Lippard, S. J. (1993) *Science 261*, 603−605.
10. McA'Nulty, M. M., and Lippard, S. J. (1996) *Mutat. Res. 362*, 75−86.
11. Chow, C. S., Whitehead, J. P., and Lippard, S. J. (1994) *Biochemistry 33*, 15124−15130.
12. Chow, C. S., Barnes, C. M., and Lippard, S. J. (1995) *Biochemistry 34*, 2956−2964.
13. Dunham, S. U., and Lippard, S. J. (1997) *Biochemistry 36*, 11428−11436.
14. Churchhill, M. E. A., Jones, D. N. M., Glaser, T., Hefner, H., Searles, M. A., and Travers, A. A. (1995) *EMBO J. 14*, 1264−1275.
15. Treiber, D. K., Zhai, X., Jantzen, H.-M., and Essigmann, J. M. (1994) *Proc. Natl. Acad. Sci. U.S.A. 91*, 5672−5676.
16. Lawrence, D. L., Engelsberg, B. N., Farid, R. S., Hughes, E. N., and Billings, P. C. (1993) *J. Biol. Chem. 268*, 23940−23945.
17. Farid, R. S., Bianchi, M. E., Falciola, L., Engelsberg, B. N., and Billings, P. C. (1996) *Toxicol. Appl. Pharmacol. 141*, 532−539.
18. Jamieson, E. R., Jacobson, M. P., Barnes, C. M., Chow, C. S., and Lippard, S. J. (1999) *J. Biol. Chem. 274*, 12346−12354.
19. Jia, Y., Kumar, A., and Patel, S. S. (1996) *J. Biol. Chem. 271*, 30451−30458.
20. Sha, M., Ferré-D'Amaré, A. R., Burley, S. K., and Goss, D. J. (1995) *J. Biol. Chem. 270*, 19325−19329.
21. Urbanke, C., and Schaper, A. (1990) *Biochemistry 29*, 1744−1749.
22. Perez-Howard, G. M., Weil, P. A., and Beechem, J. M. (1995) *Biochemistry 34*, 8005−8017.
23. Parkhurst, K. M., Brenowitz, M., and Parkhurst, L. J. (1996) *Biochemistry 35*, 7459−7465.
24. Parkhurst, K. M., Richards, R. M., Brenowitz, M., and Parkhurst, L. J. (1999) *J. Mol. Biol. 289*, 1327−1341.
25. Barawkar, D. A., and Ganesh, K. N. (1994) *Biochem. Biophys. Res. Commun. 203*, 53−58.
26. Barawkar, D. A., and Ganesh, K. N. (1995) *Nucleic Acids Res. 23*, 159−164.
27. Yamagata, A., Masui, R., Kato, R., Nakagawa, N., Ozaki, H., Sawai, H., Kuramitsu, S., and Fukuyama, K. (2000) *J. Biol. Chem. 275*, 13235−13242.
28. Pil, P. M., and Lippard, S. J. (1992) *Science 256*, 234−237.
29. Ohndorf, U.-M., Rould, M. A., He, Q., Pabo, C. O., and Lippard, S. J. (1999) *Nature 399*, 708−712.
30. Poklar, N., Pilch, D. S., Lippard, S. J., Redding, E. A., Dunham, S. U., and Breslauer, K. J. (1996) *Proc. Natl. Acad. Sci. U.S.A. 93*, 7606−7611.
31. Jadhav, V. R., Barawkar, D. A., and Ganesh, K. N. (1999) *J. Phys. Chem. B 103*, 7383−7385.
32. Drees, B. L., Rye, H. S., Glazer, A. N., and Nelson, H. C. M. (1996) *J. Biol. Chem. 271*, 32168−32173.
33. Cantor, C. R., and Schimmel, P. R. (1980) *Biophysical Chemistry*, Vol. 2, W. H. Freeman and Co., San Francisco.
34. Sjöback, R., Nygren, J., and Kubista, M. (1995) *Spectrochim. Acta, Part A 51*, L7−L21.
35. Payet, D., Hillisch, A., Lowe, N., Diekmann, S., and Travers, A. (1999) *J. Mol. Biol. 294*, 79−91.
36. Murphy, F. V., IV, Sweet, R. M., and Churchill, M. E. A. (1999) *EMBO J. 18*, 6610−6618.
37. Allain, F. H.-T., Yen, Y.-M., Masse, J. E., Schultze, P., Dieckmann, T., Johnson, R. C., and Feigon, J. (1999) *EMBO J. 18*, 2563−2579.
38. Love, J. J., Li, X., Case, D. A., Giese, K., Grosschedl, R., and Wright, P. E. (1995) *Nature 376*, 791−795.
39. Werner, M. H., Huth, J. R., Gronenborn, A. M., and Clore, G. M. (1995) *Cell 81*, 705−714.

40. Lycksell, P.-O., Gräslund, A., Claesens, F., McLaughlin, L. W., Larsson, U., and Rigler, R. (1987) *Nucleic Acids Res. 15*, 9011−9025.
41. Patel, N., Berglund, H., Nilsson, L., Rigler, R., McLaughlin, L. W., and Gräslund, A. (1992) *Eur. J. Biochem. 203*, 361−366.
42. Kopka, M. L., Yoon, C., Goodsell, D., Pjura, P., and Dickerson, R. E. (1985) *J. Mol. Biol. 183*, 553−563.
43. Kopka, M. L., Yoon, C., Goodsell, D., Pjura, P., and Dickerson, R. E. (1985) *Proc. Natl. Acad. Sci. U.S.A. 82*, 1376−1380.
44. Marky, L. A., and Breslauer, K. J. (1987) *Proc. Natl. Acad. Sci. U.S.A. 84*, 4359−4363.
45. Hsieh, M., and Brenowitz, M. (1997) *J. Biol. Chem. 272*, 22092−22096.
46. Webb, M., and Thomas, J. O. (1999) *J. Mol. Biol. 294*, 373−387.
47. Giese, K., Amsterdam, A., and Grosschedl, R. (1991) *Genes Dev. 5*, 2567−2578.
48. Yamamoto, A., Ando, Y., Yoshioka, K.-I., Saito, K., Tanabe, T., Shirakawa, H., and Yoshida, M. (1997) *J. Biochem. 122*, 586−594.
49. Patrick, S. M., and Turchi, J. J. (1998) *Biochemistry 37*, 8808−8815.
50. He, Q., Liang, C. H., and Lippard, S. J. (2000) *Proc. Natl. Acad. Sci. U.S.A. 97*, 5768−5772.
51. Kraulis, P. J. (1991) *J. Appl. Crystallogr. 24*, 946−950.

BI000342H